

## Research Article

# Sol-gel TiO<sub>2</sub> nanoparticles prompt photocatalytic cement for pollution degradation

Elena Cerro-Prada<sup>1\*</sup>, Vicente Torres Costa<sup>2</sup> and Miguel Manso Silván<sup>2</sup><sup>1</sup>Civil Engineering Department, Universidad Politécnica de Madrid, C/Alfonso XII, 3 y5, 28014 Madrid, Spain<sup>2</sup>Applied Physics Department, Universidad Autónoma de Madrid, Ciudad Universitaria de Cantoblanco, 28049, Madrid, Spain

## Abstract

TiO<sub>2</sub> nanoparticles (TiO<sub>2</sub>NPs) prepared by the sol-gel method have been incorporated to cement paste with the aim of creating a photocatalytic system capable of compensating, through degradation of hazardous molecules, the environmental impact associated to the production of the clinker. Doping was carried out at different mass ratios with TiO<sub>2</sub>NPs precursor solutions within a fresh cement paste, which was then characterized using scanning electron microscopy (SEM). The photocatalytic performance was evaluated by the degradation of Methylene Blue (MB) using a 125W UV lamp as irradiating source. Main cement properties such as hydration degree and C-S-H content are affected by TiO<sub>2</sub>NPs doping level. Cement containing TiO<sub>2</sub>NPs exhibited an increasing photocatalytic activity for increasing doping, while the pure cement paste control could hardly degrade MB. The kinetics of the system were also studied and their second order behavior related to microstructural aspects of the system.

## Introduction

In order to address the significant problem of environmental pollution, extensive research is underway to develop advanced analytical, biochemical, and physicochemical methods for the characterization and degradation of hazardous chemical compounds from air, soil, and water. Advanced physicochemical processes such as semiconductor photocatalysis have been applied to a variety of problems of environmental interest in addition to water and air purification. Several simple oxide and sulfide semiconductors, such as TiO<sub>2</sub>, ZnO or ZnS, have band-gap energies sufficient for promoting a wide range of chemical reactions of environmental interest. Among these semiconductors TiO<sub>2</sub> has proven to be the most suitable for widespread environmental applications. TiO<sub>2</sub> is biologically and chemically inert; it is stable with respect to photocorrosion and chemical corrosion; and, moreover, it is inexpensive. Despite crystallinity is not the only key factor that determines the photocatalytic performance, titanium dioxide in anatase form appears to be the most photoactive and the most practical of the semiconductors for environmental applications [1]. However, many researchers claim that amorphous titania is also a catalytically active form of TiO<sub>2</sub>, exhibiting a selective activity toward certain substrates [2,3]. This study confirms that if an appropriate porous configuration is provided, the photocatalytic activity could be higher for amorphous structures, which leads to the conclusion that microstructural aspects play a significant role as well.

In the present work, it was attempted to present the photocatalytic performance of non-condensed TiO<sub>2</sub> nanoparticles (TiO<sub>2</sub>NPs) prepared by sol-gel and inserted into the cement paste. The model dye chosen to establish the degradation capability was methylene blue (MB). The kinetics of the MB disappearance was studied. The influence of embedded TiO<sub>2</sub> precursors on the microstructure of the cementitious matrix was also analyzed.

## Experimental

### Materials

Cement paste was prepared with CEM I 42,5 ordinary Portland cement supplied by Portland Valderrivas, Madrid, Spain. The chemical composition was SiO<sub>2</sub> (20.80), Al<sub>2</sub>O<sub>3</sub> (4.40), Fe<sub>2</sub>O<sub>3</sub> (2.90), CaO (62.30), MgO (2.70), SO<sub>3</sub> (3.14) and the fineness was 1800 cm<sub>2</sub>/g. The water/cement ratio used was 0.5. Methylene blue was supplied by Sigma-Aldrich at 0.04% solution in water and used as received. Solutions were prepared using de-ionized water with an initial concentration of 18×10<sup>-6</sup> M. The photocatalyst was TiO<sub>2</sub> sol prepared from the solution of titanium isopropoxide (TTIP) (97%) purchased from Sigma-Aldrich at 0.4 M in ethanol, with a precise TTIP/water molar ratio of 0.82 and pH of 1.27 controlled with HCl. TiO<sub>2</sub>NP mean size = 14 ± 7 nm [4].

### Photoreactor and light source

The photoreactor (90 ml) had a cylindrical shape with a top optical window whose section area was ca.11 cm<sup>2</sup>, through which the suspension was irradiated. The UV-irradiation was provided by a high pressure UV 22 125 W mercury lamp (Optical Engineering) which emits radiation predominantly at 351 nm. In order to measure the absorption spectra of MB as a function of UV irradiation time, monochrome (SpectraPro 150) transmitted light was measured with an SPD-M10Avp photodiode connected to a DSP dual lock-in amplifier (7225 Signal Recovery).

**Correspondence to:** Elena Cerro-Prada, Civil Engineering Department, Universidad Politécnica de Madrid, C/Alfonso XII, 3 y5, 28014 Madrid, Spain, Tel: (+34) 91 33677 52; Fax: (+34) 91 336 79 55; **E-mail:** Elena.cerro@upm.es

**Key words:** TiO<sub>2</sub> induced photocatalysis, photocatalytic cement, cement paste microstructure, nanotechnology in cement systems

**Received:** March 20, 2016; **Accepted:** April 15, 2016; **Published:** April 20, 2016

## Procedure

Five series of TiO<sub>2</sub>NPs-cement paste were prepared. The first series (CONTROL) consisted of pure cement paste stored at 293 K in air, with no TiO<sub>2</sub> addition. The second to fifth series corresponded to cement paste mixed with TiO<sub>2</sub> sols. Four different TiO<sub>2</sub>/cement paste content ratios were used, labeled TiO<sub>2</sub>/CEM (1:10), (1:100), (1:1000) and (1:10000) according with their TiO<sub>2</sub>/cement weight ratio. All samples were 1 cm × 1 cm × 0.3 cm in size. A volume of 100 ml of the aqueous solution of MB ( $C_0 = 18 \times 10^{-6}$  M) was prepared and kept in the dark before using it. After the curing time, the cement specimens were inserted in 3 cm diameter quartz cuvettes filled with the aqueous dilution of MB. Samples were then irradiated with the UV lamp for different selected times, and their absorbance was measured.

## Results and discussion

### Photocatalytic degradation of MB in water by sol TiO<sub>2</sub>NPs/cement/UV

The photocatalytic efficiency can be established by first-order kinetic equation using the basic equation of decay

$$\ln(c/c_0) = -Kt \quad (1)$$

where  $c_0$  is the initial concentration of MB,  $c$  is the MB concentration at a given time  $t$  from which a decay constant  $K$  was calculated. This allows estimating a degradation rate calculated from fitting the kinetics of MB absorption to exponential decays. The values of the rate of degradation ( $\mu\text{Mmin}^{-1}$ ) were calculated from the kinetic data and plotted versus TiO<sub>2</sub> doping level, as shown in Figure 1. For the concentrations tested, it is observed that the degradation rate does not reach saturation for TiO<sub>2</sub>NP additions, suggesting that there are still MB molecules available for degradation if an increased number of TiO<sub>2</sub>NPs was incorporated. Thus, in the work presented herein, the degradation rate of MB increases with amount of photocatalyst without reaching a specific limit.

In order to examine the controlling mechanism of photodegradation process, the experimental data were also analyzed using the pseudo-first and pseudo-second-order kinetic models, and kinetic constants were calculated in all samples. The pseudo-first-order kinetic model has been widely used to predict dye degradation kinetics. A linear form of pseudo-first-order model was described by Lagergren

$$\log(q_e - q) = \log q_e - (k_1 / 2.303)t \quad (2)$$

where  $q_e$  and  $q$  are the amounts of photodegraded MB by the TiO<sub>2</sub>NPs/Cement system at equilibrium and at time  $t$ , respectively (mg/g) and  $k_1$  is the rate constant of first-order kinetics (1/min). The amount of photodegraded MB can be calculated from the experimental data by using the following relationship:

$$q_e = (c_0 - c_e)M \quad (3)$$

where  $c_0$  and  $c_e$  are the initial and equilibrium concentrations (mg/L) of MB, respectively, and  $M$  is the mass of TiO<sub>2</sub>NPs used. The values of first-order rate constants and the correlation coefficient  $r^2$  values obtained after the linear correlations were calculated. Although there is an initial increase in the  $k_1$  from CONTROL sample to 1:10000 samples, only moderate increases are observed as the TiO<sub>2</sub>NPs addition level increases, displaying even a lower equilibrium rate constant when the TiO<sub>2</sub>/Cement weight rate reaches 1:100 levels. We found no applicability of the pseudo-first-order model in predicting the kinetics of MB absorption degradation in the TiO<sub>2</sub>NPs doped cement paste was observed (Figure 1).

A pseudo-second-order model may also describe the kinetics of degradation. The pseudo second-order equation is based on the degradation capacity of the solid phase. This model predicts that intra-particle diffusion/transport process is the rate controlling step, which may involve valence forces through sharing or exchange of electrons between dye anions and photoreactants. The kinetic data were further analyzed using Ho's pseudo-second-order kinetics [5]

$$t/q = 1/(k_2 q_e) + (1/q_e)t \quad (4)$$

where  $k_2$  is the rate constant of second-order (1/min). If the second-order kinetic is applied, the plot of  $t/q$  against  $t$  should give a linear relationship, from which  $q_e$  and  $k_2$  can be determined from the slope and intercept of the plot. The values were calculated from the kinetic data. The fitted plots are given in Figure 1b and the calculated  $q_e$ ,  $k_2$ , and the corresponding linear regression correlation coefficient values. The smallest correlation coefficient in this case was 0.98977, which corresponds to 1:10000 TiO<sub>2</sub>/Cement weight ratio. The rest of the samples display correlation coefficients for the second-order kinetics model greater than 0.99, indicating the applicability of this kinetics equation and the second-order nature of the photodegradation process of MB in the TiO<sub>2</sub>/Cement system. This fact indicates that the rate

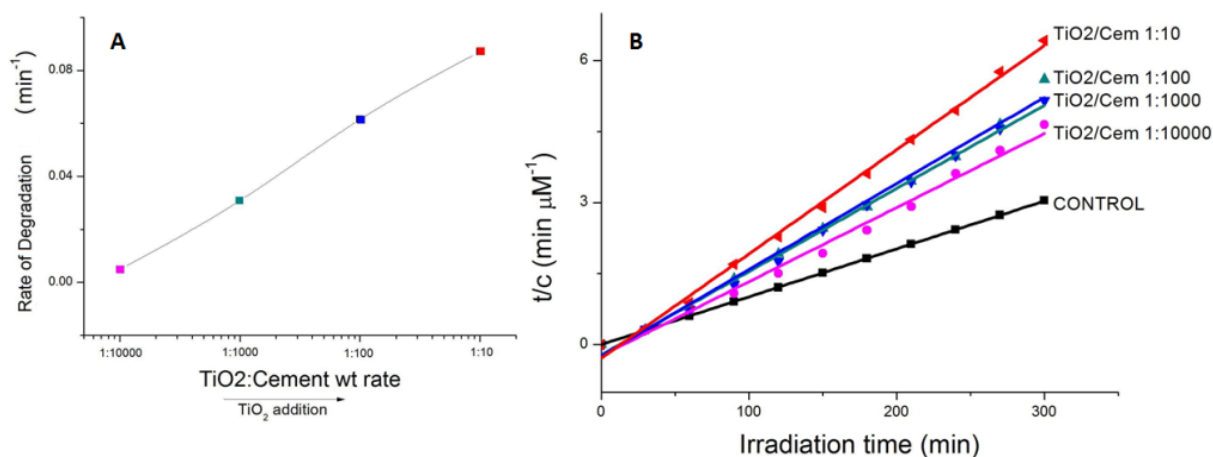


**Figure 1.** (A) Speed of MB degradation versus TiO<sub>2</sub>NPs doping level in TiO<sub>2</sub>/Cement samples. (B) Pseudo-second-order kinetics approach for MB degradation in TiO<sub>2</sub>NPs/Cement system at different addition levels.

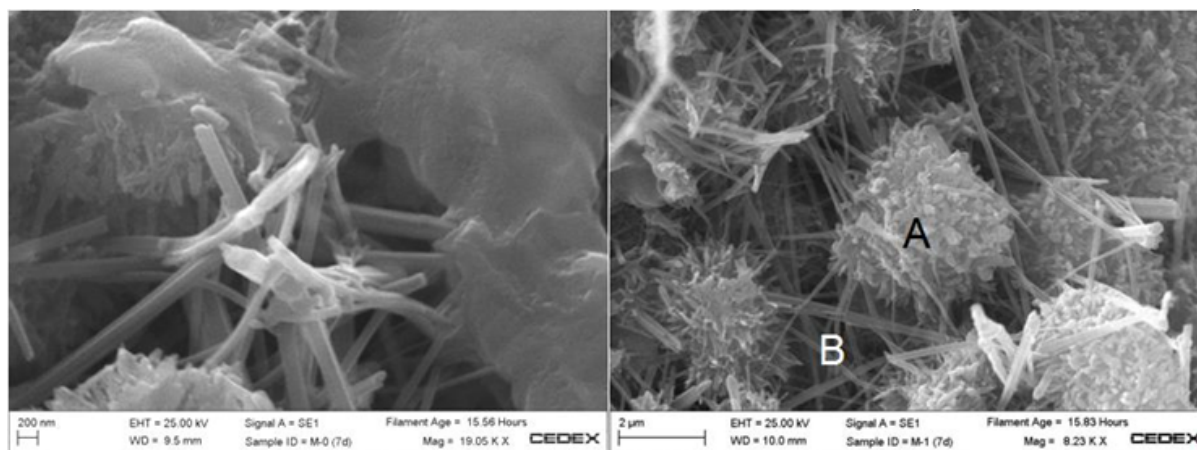


**Figure 2.** Left: Detail of SEM micrograph of the CONTROL sample after 7 days hydration time (Right) and TiO<sub>2</sub>/CEM 1:10 sample after 7 days hydration time, showing shell microspheres of amorphous inner C-S-H gel formed around a TiO<sub>2</sub> nanoparticle. Fibrillar outer C-S-H bridges the spherulites filling the intra-hydrate space.

controlling step is intraparticle diffusion, which is in fact the kinetic mechanism followed by the hydration of anhydrous particles in the cement paste at the hydration period under examination [6].

### Effects on cement microstructure

To obtain detailed information about the morphology of the TiO<sub>2</sub>NPs/Cement system, SEM images were taken after 7 days of hydration for each specimen (Figure 2).

Significant contents of microspherulites were detected in all cement pastes doped with titania nanoparticles, as those shown in Figure 2 right, not found in the CONTROL sample.

A distinction between high density inner product and low density outer product can be established. The outer product shows morphology either fibrillar or foil like, whereas the inner product forms a pack and flocculates into what is usually termed “globule flocs”. The spherulitic morphology found in TiO<sub>2</sub>NPs-cement samples, appears to be consisting of bundles of inner C-S-H gel diverging from a single TiO<sub>2</sub>NP nucleus (A). Fibrillar outer C-S-H gel (B) bridges the spherulites, developing a network-like morphology. Although such spherulites were present in all TiO<sub>2</sub>NPs/CEM samples, C-S-H gel with a foil-like morphology was observed to prevail with decreasing TiO<sub>2</sub>NPs concentration.

### Conclusions

TiO<sub>2</sub>NPs were successfully synthesized by the sol-gel method and inserted in the cement paste along with the hydration water. SEM observations revealed that sol-gel TiO<sub>2</sub>NPs were preferentially located

in the porous structure of the cement, forming nucleation centers for the C-S-H gel development. The photocatalytic activity of the TiO<sub>2</sub>NPs/cement system was measured as the relative change in the absorption of the methylene blue immersion solution. Our results clearly indicated that the TiO<sub>2</sub>NPs/cement system is photoactive and the highest photocatalytic activity was obtained under the proportion: 1 part of TiO<sub>2</sub>NPs over 10 parts of cement paste, in mass. The rate controlling step for the photocatalytic processes is intraparticle diffusion, which is in fact the kinetic mechanism followed by the hydration of anhydrous particles in the cement paste.

### References

1. Sclafani A, Herrmann JM (1996) Comparison of the photoelectronic and photocatalytic activities of various anatase and rutile forms of titania in pure liquid organic phases and in aqueous solutions. *J Chem Phys* 100: 13655-13661.
2. Cerro-Prada E, Manso M, Torres V, Soriano J (2015) Microstructural and photocatalytic characterization of cement-paste sol-gel synthesized titanium dioxide. *Frontiers of Structural and Civil Eng* 1-9.
3. Tao H J, Tao J, Wang T (2005) Fabrication of self-organized TiO<sub>2</sub> nanotubes by anodic oxidation and their photocatalysis. *Transactions of Nonferrous Metals Society of China* 15: 462.
4. Vaquero VS, Noval AM, Sánchez NT (2010) Preparation, modification and cellular evaluation of PEG-PEGd supports with titania nanoparticle loads. *Surface and Interface Analysis* 42: 481-485.
5. Vadivelan V, Kumar KV (2005) Equilibrium, kinetics, mechanism, and process design for the sorption of methylene blue onto rice husk. *J Colloid and Interface Sci* 286: 90-100.
6. Van Breugel K (1995) Numerical simulation of hydration and microstructural development in hardening cement-based materials:(II) applications. *Cement and Concrete Res* 25: 522-530.